Computers and Concrete, *Vol. 24, No. 3* (*2019*) *237-247*
DOI: https://doi.org/10.12989/cac.2019.24.3.237

Finite element modeling of bond-slip performance of section steel reinforced concrete

Biao Liu*[1] and Guo-Liang Bai[1,2,3,4]

[1]School of Civil Engineering, Xi'an University of Architecture & Technology, No. 13 Yanta Road, Xi'an, Shaanxi Province, P.R. China
[2]Key Lab of Structural Engineering and Earthquake Resistance, Ministry of Education (XAUAT), No. 13 Yanta Road, Xi'an, Shaanxi Province, P.R. China
[3]Shaanxi Key Lab of Structure and Earthquake Resistance (XAUAT), No. 13 Yanta Road, Xi'an, Shaanxi Province, P.R. China
[4]Collaborative Innovation Center for Assembled Buildings in Western China (XAUAT), No. 13 Yanta Road, Xi'an, Shaanxi Province, P.R. China

(*Received December 17, 2018, Revised June 5, 2019, Accepted July 18, 2019*)

Abstract. The key issue for the finite element analysis (FEA) of section steel reinforced concrete (SRC) structure is how to consider the bond-slip performance. However, the bond-slip performance is hardly considered in the FEA of SRC structures because it is difficult to achieve in the finite element (FE) model. To this end, the software developed by Python can automatically add spring elements for the FE model in ABAQUS to considering bond-slip performance. The FE models of the push-out test were conducted by the software and calculated by ABAQUS. Comparing the calculated results with the experimental ones showed that: (1) the FE model of SRC structure with the bond-slip performance can be efficiently and accurately conducted by the software. For the specimen with a length of 1140 mm, 3565 spring elements were added to the FE model in just 6.46s. In addition, different bond-slip performance can also be set on the outer side, the inner side of the flange and the web. (2) The results of the FE analysis were verified against the corresponding experimental results in terms of the law of the occurrence and development of concrete cracks, the stress distribution on steel, concrete and steel bar, and the P-S curve of the loading and free end.

Keywords: section steel reinforced concrete structure; bond-slip performance; finite element analysis of ABAQUS; spring element

1. Introduction

Section steel reinforced concrete (SRC) structures is widely used in high-rise building structures due to its high strength, high rigidity and good seismic performance (Nataraja *et al*. 1999, Nikolaev *et al*. 2017, Geromel and Mazzarella 2005, Chung 2000, Li *et al*. 2010, Yang *et al*. 2005, LI *et al*. 2015). The bonding effect of the two materials in the SRC structure determines the cooperative performance of section steel and concrete. Some studies had demonstrated that the bond strength of SRC is less than 50% of the bond strength between round steel bars and concrete. The weaker bond strength caused the two materials to be slippery at the interface, the slippage reduced the ability to work together, and directly influenced the strength, stiffness and applicability of the SRC structure. Therefore, the bond-slip performance of SRC has become a key issue in the research of theory of SRC structure (Li *et al*. 2010, Yang *et al*. 2005, LI *et al*. 2015). Scholars had carried out a lot of experimental research on this problem, and obtained important theories such as bond strength and bond-slip constitutive relation (Li *et al*. 2010, Yang *et al*. 2005, LI *et al*. 2015, Yang 2003, Hunaiti 1991, Roeder *et al*.1999).

These researchers have proposed that the experimental research belongs to the basic work of finite element analysis (FEA) of SRC structure. However, the current research on FEA of bond-slip performance of SRC structure is less, the work efficiency is not high enough and not accurate enough, and therefore the theory of bond-slip obtained by the test cannot be applied to FEA well. The reason is that the work of FEA of SRC structures considering bond-slip properties is very laborious and difficult, and this problem is reflected in related literature (Huang and Chen 2018, Yang 2003, Wang *et al*. 2016). For example, Huang set a larger mesh size in order to be able to manually add spring elements. Yang proposed a more complicated method to consider the bond-slip performance. Wang chose the Coulomb friction model to consider the bond-slip performance of SRC because he could not input enough spring elements, it is known from the mechanism of bond-slip that the approach is not reasonable.

The FEA of bond-slip performance can be performed using the cohesive element, the nonlinear spring element and the Coulomb friction model in ABAQUS or the nonlinear spring element in ANSYS (Combination 39) (Nematzadeh and Haghinejad 2017, Huang and Chen 2018, Wang *et al*. 2016, Xu 2013, Su *et al*. 2010, Song 2010, Yang 2003), where the nonlinear spring element is most suitable. Due to the infinite number of contact points between the section steel and concrete in the actual structure, the spring element

*Corresponding author, Ph.D. Student
E-mail: src_lb@126.com

http://www.techno-press.org/?journal=cac&subpage=8
ISSN: 1598-8198 (Print), 1598-818X (Online)

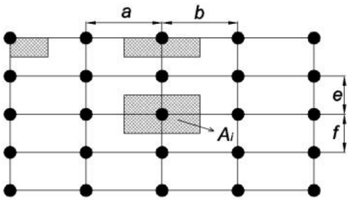

Fig. 1 The diagram of spring element area

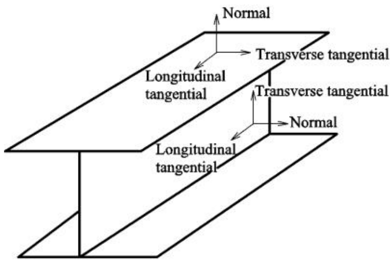

Fig. 2 Direction of section steel

should be distributed enough to accurately analyze the bond-slip performance of each interface and the stress-strain state of the section steel and concrete. Therefore, the setting of the nonlinear spring element is the key to the FEA of the bond-slip performance, the process of establishing a sufficiently fine model is complicated and error-prone. However, the existing FEA of bond-slip performance made the mesh rougher for the convenience of adding nonlinear spring elements, although the P-S curve that is consistent with the test can be obtained. Even if only one spring element is added, an accurate P-S curve can be obtained, but the practice is contrary to reality.

In order to accurately simulate the actual situation, the meshing needs to be as fine as possible, but adding large number of spring elements when the mesh is fine becomes a difficult problem. It should be emphasized that the FEA of push-out test is so difficult, and it is even more difficult to consider bond-slip performance in SRC beams, columns, joints, and structures. Apparently, the need for accuracy of FEA and the difficulty of adding enough spring element have become contradiction. The contradiction has become an obstacle to FEA considering bond-slip performance, and this obstacle causes researchers to hardly consider the bond-slip performance when performing FEA of SRC structure, which makes the existing FEA of SRC structure have defects in the modeling stage. In order to solve this problem, the software developed by Python can automatically add spring elements for the finite element (FE) model in ABAQUS to considering bond-slip performance. The methods and conclusions of this paper can not only provide reference for the FEA of SRC structures considering bond-slip performance, but also provide reference for FEA of other combined structures.

2. Overview of FEA of bond-slip performance

2.1 Element that simulates bond-slip performance

The existing literatures indicated that the elements that can be used to simulate bonding, including the spring element, the Cohesive element, the Coulomb friction model of ABAQUS and the spring element of ANSYS. The parameters of the spring element and the cohesive element are determined according to the average bond stress-slip constitutive relation (the τ-S curve) (Huang and Chen 2018, Yang 2003). Due to the powerful nonlinear analysis function of ABAQUS software (Husem *et al*. 2018, Braga *et al*. 2016), this paper chooses it as a tool for FEA of bond-slip performance. After a lot of calculations and analysis, it is found that the nonlinear spring element is most suitable, and the difference between each method to simulate the bond-slip process is as follows:

(1) The cohesive element cannot accurately describe the declining stage and horizontal residual stage of the curve.

(2) The nonlinear spring element can be used to simulate the bond-slip performance, and the F-D curve of the nonlinear spring element can be used to accurately describe the whole process of bond-slip. The reason is that the F-D curve of the spring element can be defined as the same shape as the P-S curve, including four stages: stage without deformation, rising stage, declining stage and horizontal residual stage.

(3) The Coulomb friction model has a significant defect in simulating bond-slip performance. The reason is that the bond-slip mechanism indicates that the friction force is only a part of the bond force, and it is extremely inappropriate to use the friction force instead of the bond force.

In summary, the nonlinear spring element is superior in principle to the cohesive element and the Coulomb friction model, which not only reflects the whole process of the curve but also does not need to establish a separate bonding layer, which makes the modeling more advantageous. Therefore, it is most suitable to simulate the bond-slip performance with the nonlinear spring element.

2.2 Difficulties of modeling spring element in SRC structures

2.2.1 Modeling parameters of the spring element

There are three kinds of spring elements in ABAQUS, namely Spring1, Spring2 and SpringA, Spring2 is a nonlinear spring element with two nodes, each node has only one degree of freedom. According to the actual situation, the nonlinear element is selected for FEA of the push-out test of SRC structure, and the two nodes of each element are placed on concrete and section steel, and the F-D curve of the nonlinear element is determined by the P-S relationship and is determined by the Eq. (1).

$$F = \tau * A_i \tag{1}$$

In the formula (1), F is the force of the spring element, τ is the bond stress between the section steel and the concrete, A_i is the element area around the element of the node, as shown by the shading in Fig. 1, take the middle node as an example, A_i is determined by the Eq. (2)

$$A_i = (a/2 + b/2) \times (e/2 + f/2) \tag{2}$$

Since the transverse dimension of the section steel is also large in the SRC structure, the contact action in three directions should be considered in order to meet the actual

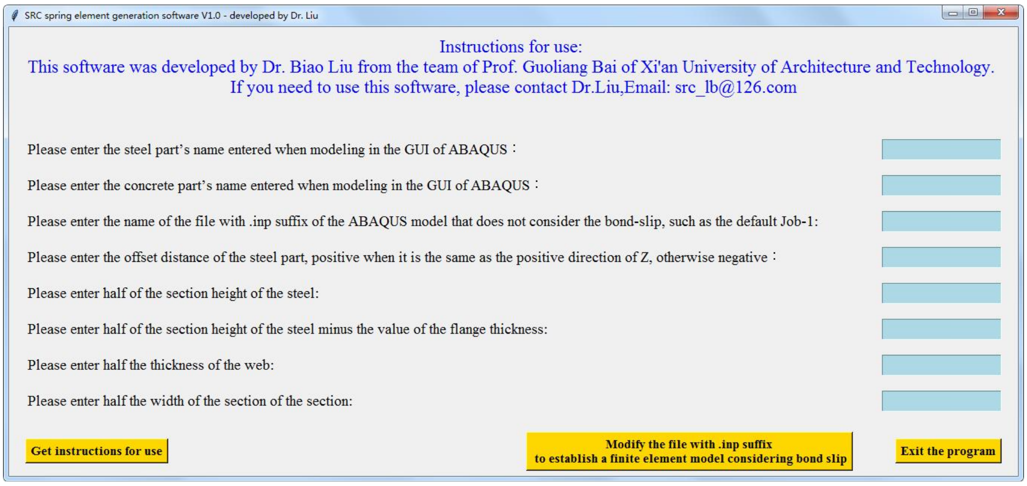

Fig. 3 SRC spring element generation software V1.0

situation. The direction definition of the section steel is shown in Fig. 2. Since the transverse tangential deformation is extremely small, this paper refers to the literature (Song 2010) to set the contact behavior of the transverse tangential direction as an elastic spring element, and the stiffness of spring element is set to the concrete elastic modulus; The contact behavior of normal direction is set to hard contact; The longitudinal tangential direction is the direction of slippage, so the nonlinear spring element is used in the longitudinal direction, and its F-D curve is determined according to the push-out test.

2.2.2 Difficulties and solutions for modeling spring elements of SRC structures

Although the nonlinear spring element is more suitable for analyzing the bond-slip performance, the researchers have been hindered by some difficulties when applying it, and these difficulties make the workload of the FE modeling considering the bond-slip performance huge, the operation is difficult and the accuracy is low.

It is necessary to find large number pairs of nodes to define the nonlinear spring element, and it is important to emphasize that one node is on concrete and the other node is on the section steel, and the coordinates of the two nodes are the same. In actual situation, the bond-slip exists at any position on the interface between the two materials. The number of spring elements to be added should theoretically be innumerable, it is necessary to establish enough spring elements. Therefore, it is extremely difficult to manually input enough pairs of nodes in the file with inp suffix as required. The specimens of push-out test with a length of 540 mm are used to illustrate the modeling difficulty of the nonlinear spring element. When the overall mesh size of the specimen is 10 mm, there are 18,810 concrete nodes and 3510 section steel nodes. There are 2,970 pairs of nodes with the same coordinates at the interface between section steel and concrete, and the process of establishing the nonlinear spring element is to randomly looking for 2970 pairs of nodes in 18,810 concrete nodes and 3510 section steel nodes. For another example, when the mesh size is 5 mm, there are 151,074 concrete nodes and 27,864 section steel nodes. The huge data makes it very difficult to manually add the spring elements. If the mesh division is finer or the spring element is applied to the actual structures, the difficulty is conceivable.

Due to the difficulty of adding nonlinear spring elements, the existing literature almost does not consider the bond-slip performance when performing FEA on SRC structure. At present, even considering the bond-slip performance is only for the push-out test, and the addition method of the nonlinear spring element is to manually find the two node's number in the GUI of ABAQUS, then manually enter the file with inp suffix. The process is difficult and error-prone, and the existing literature does not mention the use of programming methods to add spring elements.

In this paper, in order to solve the difficult of adding large number of the nonlinear spring element in the FEA of bond-slip performance of SRC, SRC spring element generation software V1.0 was developed to establish the FE model of SRC structure considering bond-slip performance.

3. Development of SRC spring element generation software V1.0

The SRC spring element generation software V1.0 developed in this paper is shown in Fig. 3. The interface is simple, while the source code of the software has more than 500 lines, and the reason is that simple interface allows researchers to easily use the software. The development basis, development ideas and usage methods of the software are discussed in detail below.

3.1 Foundation of development

The development of this software is based on the file with inp suffix generated in the modeling process in ABAQUS, and this file can be saved by the Job option of ABAQUS, which contains FE model information stored regularly, such as the name, geometry, material, mesh, element, node information, load and boundary conditions of each part. The related secondary development relies on the programming of the information in the file with inp suffix (LI and Wang 2013). The development of the SRC spring element

```
*Element, type=Spring2, elset=SpringZ_yywc
1, S-1.7, C-1.20
2, S-1.10, C-1.12
3, S-1.21, C-1.17
4, S-1.24, C-1.11
5, S-1.99, C-1.1415
6, S-1.100, C-1.1414
7, S-1.101, C-1.1413
8, S-1.102, C-1.1412
9, S-1.103, C-1.1411
10, S-1.104, C-1.1410
11, S-1.105, C-1.1409
12, S-1.106, C-1.1408
```

Fig. 4 Part of the spring element

```
*Spring, NONLINEAR, elset=SpringZ_yywc
3, 3
0, 0
52.44715, 0.001
83.93208, 0.44125
73.68185, 0.59761
69.03255, 0.91762
62.52601, 1.43812
59.05921, 2.20163
57.23038, 3.12697
57.06533, 5
57.06533, 20
```

Fig. 5 The contents of Constitutive_yywc.txt

generation software chose the Python language for three reasons: (1) Python is an object-oriented interpreted computer programming language that is easy to operate; (2) ABAQUS can directly run the file with .py suffix compiled by the Python language; (3) Python language is currently the most widely used language, which is conducive to the subsequent improvement of spring element generation software.

3.2 Development process

The logic for the development of the SRC spring element generation software V1.0 in this paper consists of three steps:

(1) Establish the FE model of the SRC specimen that does not consider the bond-slip performance, and store the model's file with inp suffix. Due to the irregularity of the section shape of the section steel, it is necessary to cut the section steel several times so that it can divide the regular mesh, thereby ensuring that the coordinates of the nodes of the section steel and the concrete are identical for defining the spring element;

(2) Based on the regular information of the FE model in the file with inp suffix, the Python language programming program is used to find the number of pairs of nodes with the same node coordinates in the section steel and concrete. And because the bond-slip constitutive relationship of different positions of the section steel is different, in this paper, these pairs of nodes are divided into three groups according to the position in the section steel: the outer side of the section steel flange, the inner side of the section steel flange and the web of section steel;

(3) Use the Python language programming program to add the node pairs to the file with inp suffix in the step (1) according to the format and position requirements of the spring element in the file with inp suffix, part of the spring element added to the file with inp suffix is shown in Fig. 4. The first column is the number of the spring element, the second column is the node of the section steel connected to the spring element, and the third column is the node of the concrete connected to the spring element. Take the first spring element "1, S-1.7, C-1.20" as an example to illustrate the format requirements of the nonlinear spring element, the "1" in the first column represents the number of spring element. The "S-1.7" in the second column represents the node numbered 7 on the section steel, and "S" is the name of the section steel in the FE model, the node number on the section steel must be preceded by "S-1." to indicate that the node is on the section steel. The "C-1.20" in the third column represents the node numbered 20 on the concrete, and "C" is the name of the concrete in the FE model, the node number on the concrete must be preceded by "C-1." to indicate that the node is on the concrete, and the coordinates of the node numbered 7 on the section steel are the same as the coordinates of the node numbered 20 on the concrete.

At the same time, the F-D relationship stored in Constitutive_yywc.txt, Constitutive_yync.txt, and Constitutive_fb.txt is respectively assigned to the spring element at the outer side of the section steel flange, the inner side of the flange and the web. For example, the content of Constitutive_yywc.txt is shown in Fig. 5, the first line indicates that the nonlinear spring element is defined here and it is defined for the spring element set named "SpringZ_yywc", and the second line indicates that the direction of the spring element is the Z direction. The content after the third line indicates a nonlinear F-D curve, where the first column represents F and the second column represents D corresponding to F. The nonlinear spring element of the longitudinal tangential direction is given a nonlinear F-D relationship.

3.3 Instructions for use

The method of using the software is as follows:

(1) Name the F-D curves of the spring element of the outer side of the flange, the inner side of the flange, and the web of section steel as Constitutive_yywc, Constitutive_yync, Constitutive_fb;

(2) Place the SRC spring element generation software V1.0, three F-D files, and the file with inp suffix in the same folder;

(3) Enter the key parameters in the interface according to the prompts.

Since the input parameter is used to find the node on the part in the file with inp suffix, the name entered here must be consistent with the part's name in the ABAQUS model, otherwise, the program will exit, this setting is to prevent input errors. After clicking the button - 'Modify the file with inp suffix', a large number of spring elements will be added to the original file with inp suffix and stored as a new file with inp suffix, and the software will name it NEWJob-1.inp by default, and FEA considering bond-slip performance can be directly performed by submitting the file named NEWJob-1.inp directly into the job.

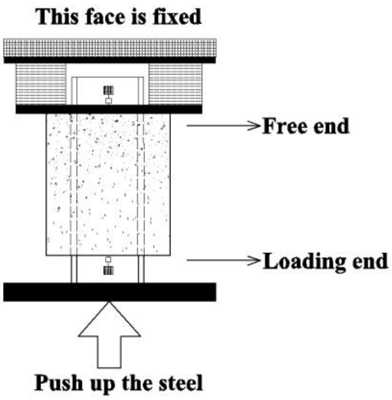

Fig. 6 Device of loading

4. FEA of the push-out test of SRC structure

In this paper, the push-out test of SRC by Yang (2003) is used to verify the reliability of the method presented. The bond-slip constitutive relation is obtained by fitting the experimental P-S curve, and there is still some error with the actual bond-slip constitutive relationship. However, the focus of this paper is to illustrate the reliability of the method presented, in order to avoid the calculation error caused by the fitting. Therefore, the relationship between the average bond stress and the slip value (τ-s relationship) of each test piece is obtained by directly processing the P-S curve. The F-D curve of the nonlinear spring element is defined according to the τ-s relationship, and with reference to the literature (Li *et al*. 2010), it is assumed that the bond-slip constitutive relations of the outer side of the flange, the inner side of the section steel flange and the web are the same. When the test is loaded, the top surface of the concrete is fixed, and the surface of section steel at the other end is pushed by the loading plate. The loading device is shown in Fig. 6, and the design of the specimens of the push-out test is shown in Table 1.

4.1 Overview of FE model

4.1.1 Element and constitutive equation of concrete

Concrete uses the C3D8R element which has 8-node (Ribeiro *et al*. 2019, Liang and Sritharan 2019, Yin and Shi 2018). Concrete Damaged Plasticity model is applied to concrete (Husem and Cosgun 2016, Kaya and Yaman 2018, Sadeghi and Hesami 2018, Dan *et al*. 2018, Nematzadeh *et al*. 2017). The constitutive equations for tension and compression are based on the elastoplastic constitutive equations considering concrete damage in the Code for Concrete Structure Design GB50010-2010.

(1) The tensile stress-strain curve of concrete is determined by the following formula

$$\sigma = (1\text{-d}_t)E_c\varepsilon \tag{3}$$

$$d_t = \begin{cases} 1-\rho_t[1.2-0.2x^5] & x \le 1 \\ 1-\rho_t/(\alpha_t(x-1)^{1.7}+x) & x > 1 \end{cases} \tag{4}$$

$$x = \varepsilon/\varepsilon_{t,r} \tag{5}$$

Table 1 Design of specimens by Yang Yong

Number	Strength		Protective layer thickness Css(mm)	Buried length Le(mm)	Stirrup information
	Design strength	Actual strength			
SRC-01	C60	44.25	40	540	A6@160
SRC-02	C60	44.25	55	740	A6@110
SRC-03	C60	44.25	70	940	A8@140
SRC-04	C60	44.25	85	1140	A8@110
SRC-05	C50	48.40	40	740	A8@165
SRC-06	C50	48.40	55	540	A8@165
SRC-07	C50	48.40	70	1140	A6@95
SRC-08	C50	48.40	85	940	A6@105
SRC-09	C40	37.20	40	940	A6@130
SRC-10	C40	37.20	55	1140	A6@140
SRC-11	C40	37.20	70	540	A8@120
SRC-12	C40	37.20	85	740	A8@120
SRC-13	C30	36.40	40	1140	A6@105
SRC-14	C30	36.40	55	940	A8@140
SRC-15	C30	36.40	70	740	A6@120
SRC-16	C30	36.40	85	540	A8@150

$$\rho_t = f_t/E_c\varepsilon_{t,r} \tag{6}$$

where α_t is The parameter value of the declining stage of the uniaxial tensile stress-strain curve of the concrete; $f_{t,r}$ is The representative value of the uniaxial tensile strength of the concrete; $\varepsilon_{t,r}$ is The peak tensile strain of the concrete corresponding to the representative value of the uniaxial tensile strength; d_t is The evolution coefficient of uniaxial tension damage of concrete.

(2) The stressed stress-strain curve of concrete is determined by the following formula

$$\sigma = (1\text{-d}_c)E_c\varepsilon \tag{7}$$

$$d_c = \begin{cases} 1-\rho_c n/(n-1+x^n) & x \le 1 \\ 1-\rho_c/(\alpha_c(x-1)^2+x) & x > 1 \end{cases} \tag{8}$$

$$\rho_c = f_c/(E_c\varepsilon_{c,r}) \tag{9}$$

$$n = E_c\varepsilon_{c,r}/(E_c\varepsilon_{c,r}-f_{c,r}) \tag{10}$$

$$x = \varepsilon/\varepsilon_{c,r} \tag{11}$$

where α_c is The parameter value of declining stage of the uniaxial compressive stress-strain curve of concrete; $f_{c,r}$ is The representative value of the uniaxial compressive strength of concrete; $\varepsilon_{c,r}$ is The peak compressive strain of concrete corresponding to the representative value of uniaxial compressive strength; d_c is The uniaxial compression damage evolution coefficient of concrete.

4.1.2 Element and constitutive equation of section steel

The C3D8R element is also used for section steel because the thickness of the section steel flange (10.6 mm) and the thickness of the web (14 mm) are both larger than the

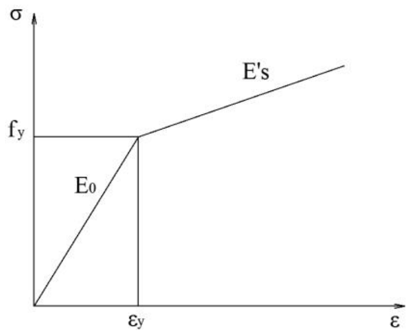

Fig. 7 Stress-strain curve of section steel and steel bar

element size (5 mm). The T3D2 element is used for steel bars, and the interaction with concrete is considered by the embedded element (Chou and Wu 2019, Sayyar *et al*. 2019, Alogla and Kodur 2018), the elastic-isotropic plastic hardening material model (Cui *et al*. 2019, Yuan *et al*. 2019) is used for section steel and steel bars, as shown in Fig. 7.

4.1.3 Key technologies for modeling

In order to save the calculation cost, and the cross section of the section steel has two axes of symmetry, and therefore only 1/4 of the model is built in the modeling. The end face of concrete at the free end is coupled with the reference point 1, and impose a constraint of 6 directions on the reference point 1. The end face of the section steel at the loading end is coupled to the reference point 2, and a constraint of 5 directions (Free in the Z direction) is applied to the reference point 2, and a displacement load is applied in the longitudinal direction. The overall model is displayed by the symmetry function of ABAQUS when viewing the calculation results. In addition, the section steel and concrete must be cut to ensure that the nodes of the two parts can be completely overlapped during the meshing, so that the spring element can be easily added.

4.2 The advantages of the method

In this paper, SRC04 is taken as an example to illustrate the superiority and reliability of the SRC spring element generation software V1.0 in modeling. The 1/4 FE model of the specimen is shown in Fig. 8, where the Fig. 8(a) is a geometric model and the Fig. 8(b) is a diagram of the mesh division, Fig. 8(c)-(d) is diagram of the deformed spring element (red curve in the figure). Since the length of the spring element is 0, the spring element after deformation is used for displaying the spring element in the model.

The lateral mesh size of the 1/4 model of the SRC04 specimen is set to 5 mm, and the longitudinal mesh size is set to 10 mm. The concrete in the model has 90045 nodes, and the section steel in the model has 8100 nodes, there are 3565 pairs of nodes with the same coordinates in the position where the section steel is in contact with the concrete. In the hardware environment where the computer memory is 8G and the processor is i5, it takes only 6.46s to perform secondary processing on the file with inp suffix of the FE model using the SRC spring element generation software V1.0, and in such a short time, 3565 pairs of nodes are automatically found, and 3565 spring elements are added in

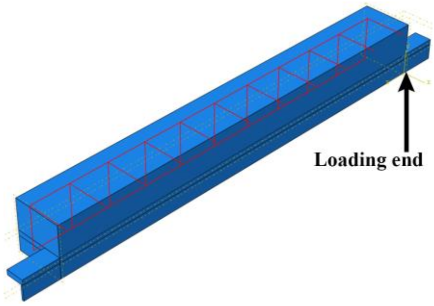

(a) Geometric model of SRC04（1/4 model）

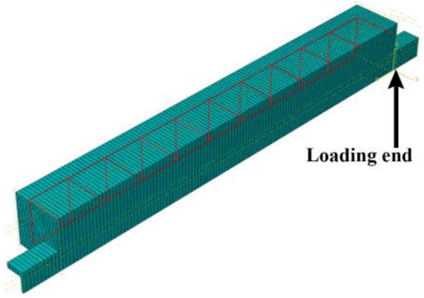

(b) FE model of SRC04（1/4 model）

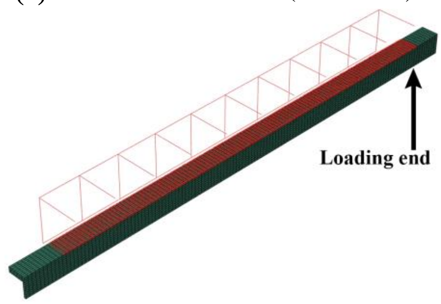

(c) Diagram of the spring element (red short curve on the section steel surface)

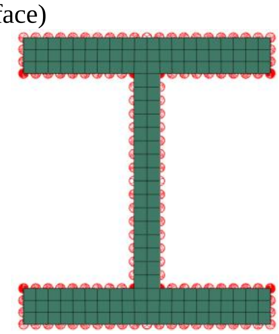

(d) Diagram of the spring element (red short curve on the section steel surface)

Fig. 8 The FE model of SRC04

the Job-1.inp file according to the format requirements, and the modeling work considering the bond-slip of SRC04 is completed, and the FE model was saved in the file named NEWJob-1.inp. The file named NEWJob-1.inp can be submitted and calculated directly in the ABAQUS Job module. The software takes up very little CPU when adding the spring element, and does not affect the computer to perform other heavy work such as calculation of ABAQUS.

The application of the example shows that the SRC spring element generation software V1.0 developed in this paper can effectively establish the FE model considering the bond-slip performance. It is found that the probability of

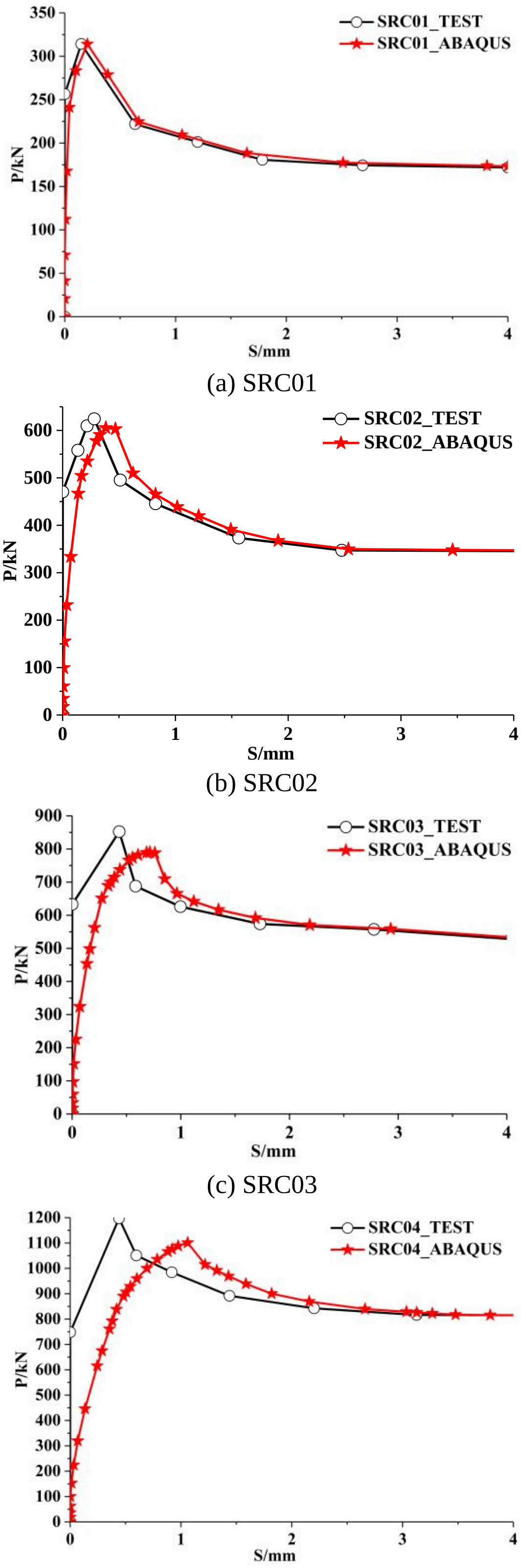

(a) SRC01
(b) SRC02
(c) SRC03
(d) SRC04

Fig. 9 P-s curves by the test and ABAQUS

error is 0 regardless of the number of nodes by randomly reviewing the different specimens with different mesh sizes and judging whether the coordinates of the two nodes of the spring element are completely consistent.

4.3 Comparison of results of FEA and push-out test

4.3.1 Comparison of P-S curves at the loading end

The FE model of the 16 specimens established by the above method was calculated in ABAQUS and compared with the results of the push-out test. The P-S curve of the loading end of each specimen calculated by ABAQUS was compared with the P-S curve of the loading end measured by the test, as shown in Fig. 9.

It can be seen from Fig. 9 that the FEA can accurately simulate the relationship between load and slip during the bond-slip process of SRC structures, and there is a certain error between the results of ABAQUS and test before the horizontal residual stage. The reason is that there are two hypotheses in the FEA of this paper: (1) The F-D relationship of the springs on the inside, outside of the flange and the web is the same. (2) The FEA of this paper does not consider the change of the F-D relationship of with the position. Short specimens are less affected by positional changes, while longer specimens are more affected. Therefore, the error of the shorter test piece is smaller, and the error of the longer test piece is larger. And the deformation of the spring element of the loading end and the free end are not uniform when the slip value is small, the spring element of the loading end has the largest deformation, and the deformation of the spring element at the free end is the smallest, which results in the force of the spring element calculated by the ABAQUS before the horizontal residual stage is smaller than the actual bond force, and the larger the embedding length, the larger the calculation error, as shown in Fig. 9, the lengths of SRC1, SRC6, SRC11, and SRC16 are the shortest, so the whole process of the P-S curve calculated by the test and ABAQUS is basically the same, while the calculation error of other specimens increases with the increase of the length. Therefore, it is necessary to propose a more accurate bond-slip constitutive relationship considering position change to solve this problem.

4.3.2 Comparison of P-S curves of the loading and free end by ABAQUS

The P-S curves of the loading end and the free end calculated by ABAQUS are shown in Fig. 10.

It can be seen from Fig. 11 that the P-S curves of the loading end and the free end are different in the rising stage and the declining stage, and are the same in the horizontal residual stage, which is also in accordance with the results of test. The reason is also the stress and deformation of the spring element at the loading end is greater than the free end before the horizontal residual stage, and the difference between the loading end and the free end increases with the length of the embedded length. And for each specimen of push-out test, as the load increases, the deformation of the spring element of the loading end and the free end become closer and closer, and are equal in the horizontal residual stage.

4.3.3 Stress comparison

The stress cloud of the section steel of SRC04 calculated by ABAQUS at peak load is shown in Fig. 11. Here, the 1/4 model is shown as a 1/2 model by symmetry.

It can be seen from Fig. 11 that the stress of the section

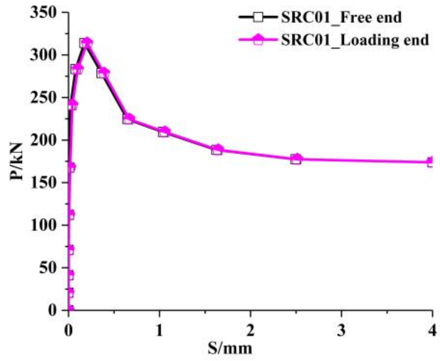

(a) SRC01

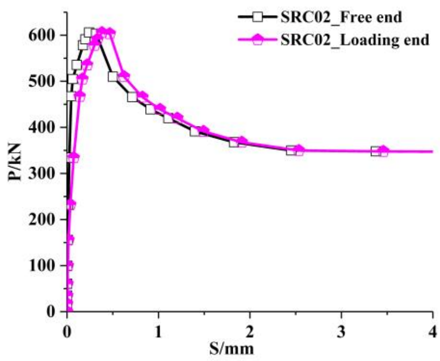

(b) SRC02

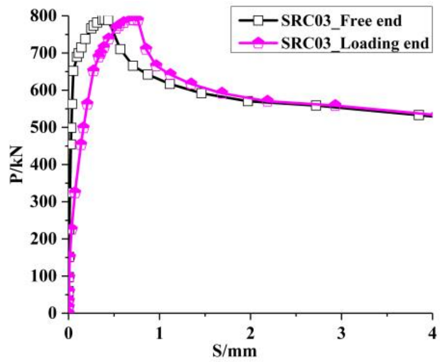

(c) SRC03

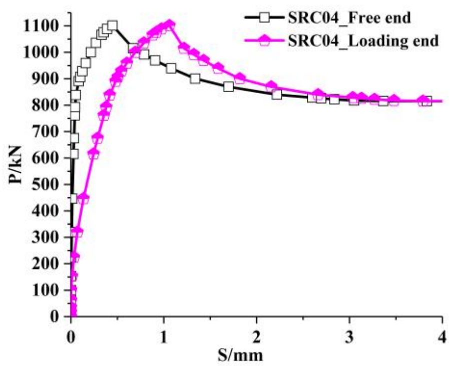

(d) SRC04

Fig. 10 The p-s curve of the loading and free end by ABAQUS

steel gradually decreases from the loading end to the free end, which is consistent with the results of test, and the stress at the loading end is mainly caused by the external load. The free end is the farthest from the loading end, so it is least

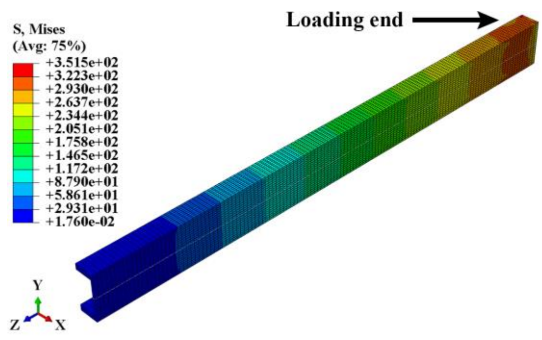

Fig. 11 Stress of section steel of SRC04

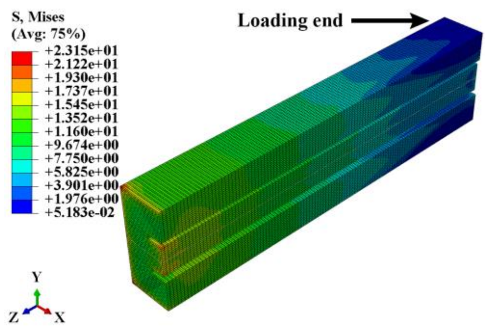

Fig. 12 Stress of concrete of SRC04

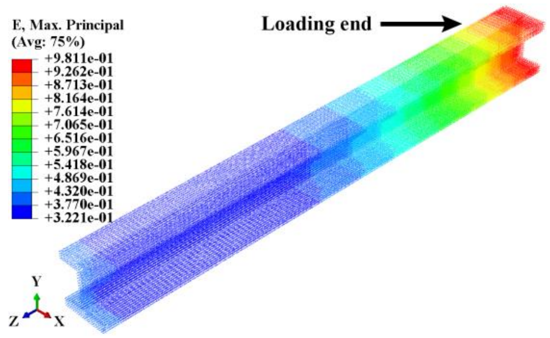

Fig. 13 Stress of concrete and spring element of SRC01

affected by the external load, and the stress here is almost caused by the bond stress, and the maximum stress of the section steel is 351.5MPa, which appears at the exposed section steel.

Fig. 12 is the stress cloud diagram of concrete of SRC04 calculated by ABAQUS at the peak load moment, where the 1/4 model is shown as a 1/2 model using symmetry. It can be seen from Fig.12 that the concrete stress gradually increases from the loading end to the free end, and the maximum value is 23.15MPa at the free end of the concrete, which is consistent with the results of test.

Fig. 13 is the strain cloud diagram of spring element of the SRC04 calculated by ABAQUS at the peak load moment. Here, the 1/4 model is shown as a complete model by symmetry. It can be seen from Fig. 14 that the distribution of strain of the spring element is not uniform, and gradually decreases from the loading end to the free end, which is caused by the large bonding stress at the loading end.

Fig. 14 is the stress cloud diagram of the steel bar. It can be seen from the figure that the steel bar has obvious tensile behavior in the X direction and increases with the increase of

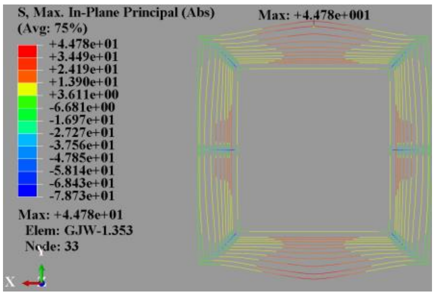

Fig. 14 Stress of the steel bar

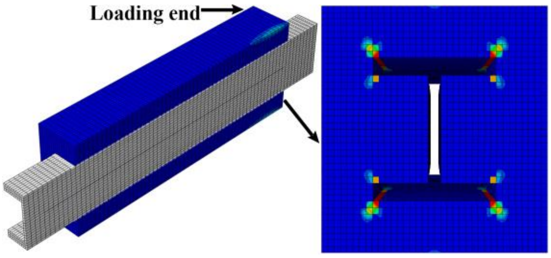

(a) SRC01

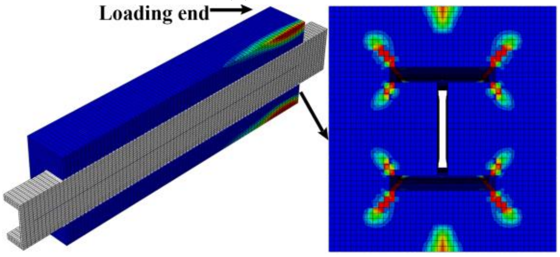

(b) SRC02

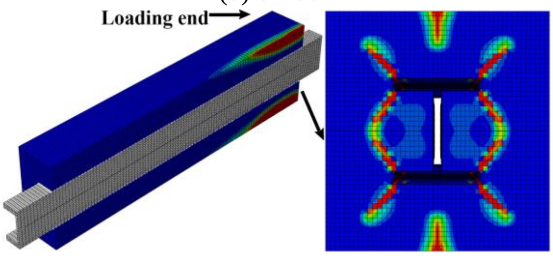

(c) SRC03

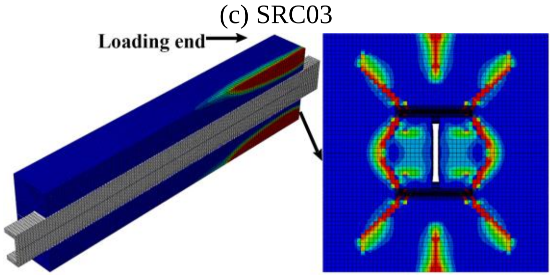

(d) SRC04

Fig. 15 The tensile damage cloud diagram (DEMAGET) of each specimen

the concrete crack width. It is due to the restraining effect between the steel bar and the concrete, which causes it to be pulled.

After analysis of the whole process of calculation, it was found that the stress of section steel and concrete was small at the initial stage of loading. As the load increases, the stress of concrete and section steel increases gradually, which is the result of the increase of the bond stress, and the stress on the concrete is caused by the bond stress generated by the load; When the load reaches the peak load, the stress and strain of the section steel and concrete also reach a peak, because the bond stress reaches the bond strength at this time; In the late stage of loading, the load decreases but the displacement increases. After the declining stage, the load remains unchanged, at this stage, the chemical adhesion completely disappears, and the bonding stress consists of friction and mechanical occlusion. The above analysis shows that the SRC FE model considering the bond-slip established by the SRC spring element generation program can accurately simulate the whole process of push-out test of the SRC.

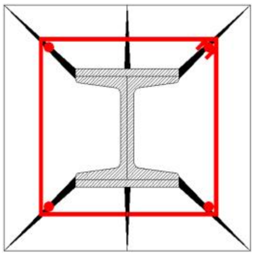

(a) The first type

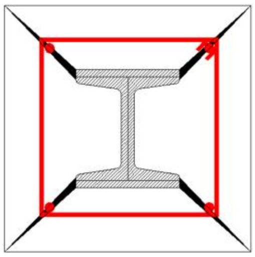

(b) The second type

Fig. 16 The fracture morphology observed in push-test

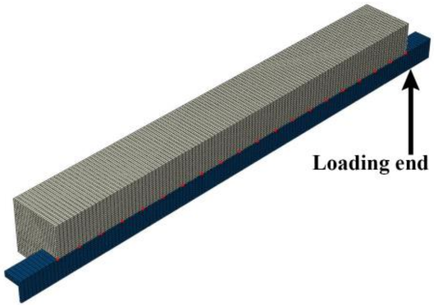

Fig. 17 The longitudinal tangential joints at the interface

4.3.4 Comparison of cracking patterns of concrete

In order to show the development of cracks, the tensile damage (DEMAGET) cloud diagram was used for showing the cracking pattern of concrete in this paper (Ren and Fan 2017). The fracture pattern of the concrete outside the section steel flange and the end face at the loading end calculated by ABAQUS is shown in Fig. 15, and the fracture morphology obtained by push-test is shown in Fig. 16.

It can be seen from Fig. 15 that the crack of the concrete develops from the middle of the section steel flange of the loading end to the free end, and the crack at the end face of the loading end is developed from the four corners of the flange of the section steel to the four corners of the concrete. The results of ABAQUS are consistent with the results of the push test in Fig. 16. The above comparison also shows that the FE method used in this paper can accurately simulate the crack pattern of concrete during the push-out test.

From the above comparison, the FEA of this paper has been verified by many aspects, including P-S curve, stress and strain distribution law and cracking mode.

4.3.5 Comparison of distribution of longitudinal strain

In order to compare the change of the bond stress

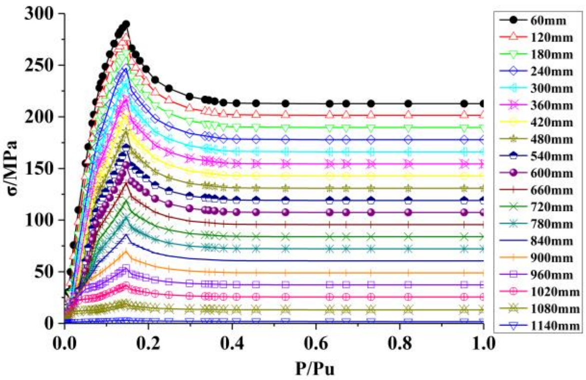

(a) section steel

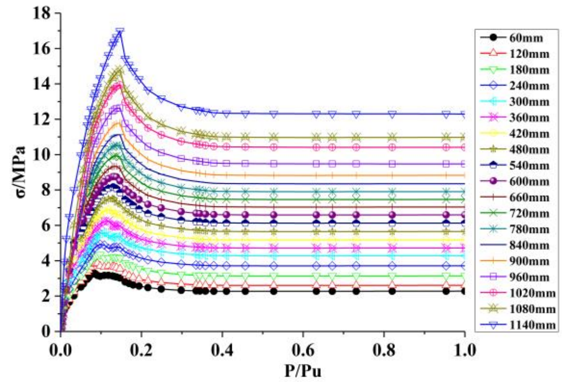

(b) concrete

Fig. 18 The variation of the stress of the nodes at different distances from the loading end with the load

between the section steel and the concrete along the loading direction (longitudinal direction), take SRC04 as an example, a set of nodes along the loading direction be selected on the section steel or concrete for analysis, as shown in Fig. 17 (red point). The stress values of the nodes in Fig. 17 at different loading moments are plotted as curves, as shown in Fig. 18.

It can be seen from Fig. 18(a) that the stress of the section steel at the interface decreases as the distance from the loading end increases, and it can be seen from Fig. 18(b) that the concrete stress at the interface increases as the distance from the loading end increases, and the stress of both parts increases with the increase of the load and decreases with the decrease of the load. The stress of the section steel and concrete at the contact surface consists of friction, bite force and chemical adhesion before the horizontal residual phase. After the disappearance of the chemical adhesion in the horizontal residual stage, the bond force is composed entirely of friction and bite force. The above conclusions are consistent with the results of the push-out test.

5. Conclusions

(1) Nonlinear spring element in ABAQUS can be used to accurately simulate the bond-slip performance of SRC structures if enough spring elements can be added;
(2) The spring element can be efficiently, accurately and simply added by the SRC spring element generation software V1.0, thereby establishing a FE model considering the bond-slip performance. For the 1/4 model, when the mesh size is 5mm and the spring element reaches 3565, the modeling can be completed with only 6.46s;
(3) The outer side of the section steel flange, the inner side of the flange and the web can be respectively added with different spring elements by the SRC spring element generation software V1.0;
(4) The bond-slip performance of the SRC structure can be accurately simulated by the method proposed in this paper, such as the P-S curves of the loading and free end, the stress of steel and concrete, and the tendency of concrete cracking.

Acknowledgement

The work in this paper was supported by the National Natural Science Foundation of China (51878544 and 51478381), this support is gratefully acknowledged.

References

Alogla, S. and Kodur, V.K.R. (2018), "Quantifying transient creep effects on fire response of reinforced concrete columns", *Eng. Struct.*, **174**, 885-895. https://doi.org/10.1016/j.engstruct.2018.07.093.

Braga, F., Marcela, B. and Greco, M. (2016), "Topological optimization procedure considering nonlinear material behavior for reinforced concrete designs", *Comput. Concrete*, **17**(1), 141-156. http://dx.doi.org/10.12989/cac.2016.17.1.141 141.

Chou, C. and Wu, S. (2019), "Cyclic lateral load test and finite element analysis of high-strength concrete-filled steel box columns under high axial compression", *Eng. Struct.*, **189**, 89-99. https://doi.org/10.1016/j.engstruct.2019.03.052.

Chung, D.D.L. (2000), "Corrosion control of section steel-reinforced concrete", *J. Mater. Eng. Perform.*, **9**(5), 585-588. https://doi.org/10.1361/105994900770345737.

Cui, Y., Luo, Y. and Nakashima, M. (2013), "Development of steel beam-to-column connections using SFRCC slabs", *Eng. Struct.*, **52**, 545-557. https://doi.org/10.1016/j.engstruct.2013.03.021.

Dan, S., Chaudhary, M. and Barai, S.V. (2018), "Punching shear behavior of recycled aggregate concrete", *Comput. Concrete*, **21**(3), 321-333. https://doi.org/10.12989/cac.2018.21.3.321.

Geromel, M. and Mazzarella, O. (2005), "Experimental and analytical assessment of the behavior of stainless section steel reinforced concrete beams", *Mater. Struct.*, **38**(2), 211-218. https://doi.org/10.1007/BF02479346.

Huang, C.X. and Chen, H. (2018), "Finite element analysis of section steel reinforced concrete member considering interface SLIP", *Steel Constr.*, **33**(2), 68-72. http://dx.doi.org/10.13206/j.gjg201802013.

Hunaiti, Y.M. (1999), "Bond strength in battened composite columns", *J. Struct. Eng.*, **117**(3), 699-714. https://doi.org/10.1061/(ASCE)0733-9445(1991)117:3(699).

Husem, M. and Cosgun, S.I. (2016), "Behavior of reinforced concrete plates under impact loading: different support conditions and sizes", *Comput. Concrete*, **18**(3), 389-404. http://dx.doi.org/10.12989/cac.2016.18.3.389 389.

Husem, M., Cosgun, S.I. and Sesli, H. (2018), "Finite element analysis of RC walls with different geometries under impact loading", *Comput. Concrete*, **21**(5), 583-592.

https://doi.org/10.12989/cac.2018.21.5.583.
Kaya, M. and Yaman, C. (2018), “Modelling the reinforced concrete beams strengthened with GFRP against shear crack”, *Comput. Concrete*, **21**(2), 127-137. https://doi.org/10.12989/cac.2018.21.2.127.
Li, H.W. and Wang, W.D. (2013), “Application of ABAQUS secondary development in finite element analysis of concrete-filled section steel tubular structures”, *J. Build. Struct.*, **34**(S1), 353-358. http://dx.doi.org/10.14006/j.jzjgxb.2013.s1.053.
Li, J.H., Li, Y.S. and Wang, J.M. (2010), “Bond-slip constitutive relation and bond-slip resilience model of shape-section steel reinforced concrete columns”, *China Civil Eng. J.*, **43**(3), 46-52. http://dx.doi.org/10.15951/j.tmgcxb.2010.03.009.
Li, J.H., Qiu, D.L. and Yu, K. (2015), “Study on bond-slip behavior between spaped section steel and concrete in SRC structures after exposed to high temperature”, *Eng. Mech.*, **32**(2), 190-200. http://dx.doi.org/10.15951/j.tmgcxb.2010.03.009.
Liang, X. and Sritharan, S. (2019), “Effects of confinement in square hollow concrete column sections”, *Eng. Struct.*, **191**, 526-535. https://doi.org/10.1016/j.engstruct.2019.04.034.
Nataraja, M.C., Dhang, N. and Gupta, A.P. (1999), “Stress–strain curves for section steel-fiber reinforced concrete under compression”, *Cement Concrete Compos.*, **21**(5), 383-390. https://doi.org/10.1016/S0958-9465(99)00021-9.
Nematzadeh, M. and Haghinejad, A. (2017), “Analysis of actively-confined concrete columns using prestressed steel tubes”, *Comput. Concrete*, **19**(5), 477-488. https://doi.org/10.12989/cac.2017.19.5.477.
Nikolaev, V.B., Lisichkin, S.E. and Rubin, O.D. (2017), “Steel-reinforced concrete penstock experiments”, *Power Technol. Eng.*, **50**(5), 466-472. https://doi.org/10.1007/s10749-017-0734-y.
Ren, X.D. and Fan, W.D. (2017), “Damage model based numerical study for shear failures of reinforced concrete beams”, *Eng. Mech.*, **34**(S1), 139-142. http://dx.doi.org/10.6052/j.issn.1000-4750.2016.03.S024.
Ribeiro, F., Sena-Cruz, J., Branco, F.G. and Júlio, E. (2019), “3D finite element model for hybrid FRP-confined concrete in compression using modified CDPM”, *Eng. Struct.*, **190**: 459-479. https://doi.org/10.1016/j.engstruct.2019.04.027.
Roeder, C.W., Chmielowski, R. and Brown, C.B. (1999), “Shear connector requirement for embedded section steel sections”, *J. Struct. Eng.*, **125**(2), 142-151. https://doi.org/10.1061/(ASCE)0733-9445(1999)125:2(142).
Sadeghi, V. and Hesami, S. (2018), “Finite element investigation of the joints in precast concrete pavement”, *Comput. Concrete*, **21**(5), 547-557. https://doi.org/10.12989/cac.2018.21.5.547.
Sayyar Roudsari, S., Hamoush, S.A., Mohamad Soleimani, S. and Madandoust, R. (2019), “Evaluation of large-size reinforced concrete columns strengthened for axial load using fiber reinforced polymers”, *Eng. Struct.*, **178**, 680-693. https://doi.org/10.1016/j.engstruct.2018.09.071.
Schultz, A.E., Mercan, B. and Stolarski, H.K. (2016), “Arc-length and explicit methods for static analysis of prestressed concrete members”, *Comput. Concrete*, **18**(1), 1-21. http://dx.doi.org/10.12989/cac.2016.17.6.000000.
Song, T.Y. (2010), “Research on post-fire performance of steel-concrete composite beam-column joints”, Ph.D., Dissertation, Tsinghua University, Beijing.
Su, X.T., Yang, Z.J. and Liu, G.H. (2010), “Finite element modeling of complex 3D static and dynamic crack propagation by embedding cohesive elements in ABAQUS”, *Acta Mechanica Solida Sinica*, **2010**(3), 271-282. https://doi.org/10.1016/S0894-9166(10)60030-4.
Wang, G.Y., Liu, Q. and Zhang, D.M. (2016), “A finite element model for post-fire seismic performance of section steel reinforced concrete columns”, *Eng. Mech.*, **33**(11), 183-192. http://dx.doi.org/10.6052/j.issn.1000-4750.2015.06.0472.
Xu, K.C. (2013), “Study on bond-slip relationship of concrete-filled steel tube based on interface damage”, Ph.D., Dissertation, Nanchang University, Nanchang.
Yang, Y. (2003), “Study on the basic theory and its application of bond-slip between steel shape and concrete in SRC stucturesS”, Ph.D., Dissertation, Xi’an University of Architecture and Technology, Xi’an.
Yang, Y., Guo, Z.X. and Xus, J.Y. (2005), “Experiment study on bond-slip behavior between section steel and concrete in SRC structures”, *J. Build. Struct.*, **26**(4), 1-9. http://dx.doi.org/10.14006/j.jzjgxb.2005.04.001.
Yin, H. and Shi, G. (2018), “Finite element analysis on the seismic behavior of fully prefabricated steel frames”, *Eng. Struct.*, **173**, 28-51. https://doi.org/10.1016/j.engstruct.2018.06.096.
Yuan, F., Wu, Y. and Li, C. (2017), “Modelling plastic hinge of FRP-confined RC columns”, *Eng. Struct.*, **131**, 651-668. https://doi.org/10.1016/j.engstruct.2016.10.018.
Zhao, H.T., Yang, Y. and Xue, J.Y. (2013), “A review on the bond-slip mechanical behaviors of SRC structures”, *Adv. Mech.*, **33**(1), 74-86. http://dx.doi.org/10.3321/j.issn:1000-0992.2003.01.009.

CC